PROTONS AS A SCREEN FOR DISPLACEMENT DAMAGE IN BIPOLAR JUNCTION TRANSISTORS

By

Charles Nathan Arutt

Thesis

Submitted to the Faculty of the

Graduate School of Vanderbilt University

in partial fulfillment of the requirements

for the degree of

MASTER OF SCIENCE

in

Electrical Engineering

December, 2014

Nashville, Tennessee

Approved:

Dr. Ronald D. Schrimpf

Dr. Robert A. Weller

Acknowledgements

For this work, I would like to thank my professors for their guidance in my academic growth and research pursuits. Specifically, I would like to thank Dr. Ron Schrimpf for his guidance and patience from my freshman year of undergrad through graduate school at Vanderbilt. I would also like to thank other members of the Electrical Engineering faculty in the Radiation Effects and Reliability group of Vanderbilt University including Professors Robert Weller, Robert Reed, Dan Fleetwood, Tim Holman, Lloyd Massengill and Bharat Bhuva, as well as Kevin Warren, Andrew Sternberg, Scooter Ball, and Jason Rowe. Thank you to Mike McCurdy and Enxia Zhang for helping run these experiments and thank you to Lewis Saettel for access to supplies and extra support.

I would also like to thank my friends and family. First, I thank my mother and father, Karen Stromberg and Paul Arutt, who have been supportive from the beginning and helped grow my curiosity of this world. A special thanks goes to Dr. Alan Tipton for his mentoring at my internship at C.S. Draper Labs and beyond. I must also thank my electrical engineering friends from Vanderbilt University. From the Graduate School, in no particular order of importance, thank you to Mike King, Nelson Gaspard, Geoff Bennett, Nick Hooten, Stephanie Weeden-Wright, Paula Chen, Zac Diggins, Isaak Samsel, Erik Funkhouser, Jeff Maharrey, and Rachel Quinn. From undergrad, thank you to Joseph Souter.

A special thank you goes to Alexandria Hamm for her love and support while writing this thesis. And finally, thank you to Conrad Miszuk for getting me to build guitar pedals in high school and making me realize that I wanted to be an electrical engineer.

Financial support for this work was provided in part by the U.S. Air Force.

Table of Contents

Page

Acknowledgements ii

List of Figures iv

List of Tables vi

Introduction 1

1.0 Review of Mechanisms 3

1.1 Displacement Damage 3
1.1.1 Effects in BJTs 7
1.2 Total Ionizing Dose 9
1.2.1 NPN BJT Mechanisms 10
1.2.2 PNP BJT Mechanisms 12

2.0 Effects of Proton Irradiation 15

2.1 Correlating Protons for Displacement Damage 15
2.2 NIEL for Protons 16
2.3 Effects of Simultaneous Displacement and Ionization Damage 17

3.0 Experimental Results 20

3.1 Experimental Details 20
3.2 Comparison of Proton and X-ray Data 23
3.3 Correlating Ionization and Displacement Damage 29
3.4 Comparison with Existing Work 34

Conclusions 35

References 36

List of Figures

Page

Figure 1-1: Spatial distribution of initial defect configuration due to primary knock on atom for proton irradiation, after [14]. 4

Figure 1-2: Reciprocal gain vs. fluence for sequential irradiation of the same 2N2222A NPN transistor with 16.8 MeV and 40.0 MeV helium ions and 4.3 MeV deuterons, after [16]. The slope, or damage factor changes for each type of ion. 6

Figure 1-3: Displacement damage factor as a function of collector current for an NPN and PNP transistor with neutrons, 65 MeV helium ions, and 3.7 MeV protons, after [16]. 6

Figure 1-4: Gummel plot for a 2N2222 BJT pre and post neutron irradiation, after [21]. 8

Figure 1-5: Cross section of a typical NPN BJT. The dashed line represents the area most sensitive to ionizing radiation, after [4]. 8

Figure 1-6: Normalized current gain versus base-emitter voltage for increasing levels of total ionizing dose, after [12]. 11

Figure 1-7: Excess base current versus base-emitter voltage for various levels of total ionizing dose with an ideality factor of 2 super imposed for comparison, after [12]. 11

Figure 1-8: A diagram of a generic vertical PNP transistor showing how the depletion region narrows in the n-type base due to positive oxide charge, after [4]. 13

Figure 1-9: A diagram of a lateral PNP transistor showing current flow under oxide, after [4]. 13

Figure 1-10: Normalized current gain vs. total dose from lateral (LPNP), substrate (SPNP), and vertical (VPNP) BJTs [9]. 14

Figure 1-11: Normalized current gain vs. emitter-base voltage from lateral (LPNP), substrate (SPNP), and vertical (VPNP) BJTs at a dose of 500 krad(SiO_2) [9]. 14

Figure 2-1: Linear relationship between measured damage factors for 2N2222A transistors and calculated NIEL for protons. Corresponding proton energy is shown at the top [16]. 16

Figure 2-2: Change in LM124 bias current versus equivalent fluence for X-ray (ionization), neutron (displacement), and proton irradiations, after [28]. 18

Figure 2-3: Analytically calculated ratio of X-ray to proton radiation response based on depth and doping of the device base, after [29]. 19

Figure 3-1: Cross section of BJTs in Intersil's BiCMOS process [37]................................. 20

Figure 3-2: Gummel plot of a PNP device irradiated with 4 MeV protons. Note the increasing current base current as the radiation increases.. 24

Figure 3-3: Gummel plot of a PNP device irradiated with 10 keV X-rays. Note the much smaller magnitude of excess base current.. 24

Figure 3-4: Beta plot of a PNP device. Note the decreasing gain as the radiation increases. 26

Figure 3-5: Reciprocal gain plot of four PNP devices the same size. There is a linear increase for both the proton and X-ray irradiated parts. The slope of these lines is the damage factor at this bias. 27

Figure 3-6: Reciprocal gain plot of four NPN devices the same size. Note the slopes are similar to the values in Figure 3-5. The last data point for NPN 11 is omitted due to device failure.. 27

Figure 3-7: NPN BJT damage factors at 0.6 V V_{BE} bias. 28

Figure 3-8: PNP BJT damage factors at 0.6 V V_{BE} bias... 28

Figure 3-9: Damage factors for four NPN and four PNP devices that are similarly sized..... 30

Figure 3-10: Mass-stopping powers versus particle energy for protons, electrons, and secondary electrons generated by 10 keV X-rays and 1.25 MeV Co-60 gamma ray photons. Shaded area corresponds to proton energies used by Schwank *et al*. and proton and electron data are from Oldham *et al* [13], [36]....................................... 31

Figure 3-11: Charge yield for protons compared to proton energy. Shaded area corresponds to proton energies used by Schwank *et al*. and original plot from Oldham *et al* [13], [36]. For the charge yield experiments, n-channel transistors were irradiated with the gates grounded. 31

Figure 3-12: Damage factor ratio with charge yield correction factor for similarly sized NPN and PNP BJTs. 33

Figure 3-13: Damage factors for the same four NPN and four PNP BJTs as shown in Figure 1-3 using collector current as the abscissa for easy comparison to the similar plot from Summers et al.[16]. 33

List of Tables

Page

Table 2-1: NIEL Values for 4 MeV protons Calculated by Different Methods 17

Table 3-1: PNP BJT to NPN BJT Ratio for Each Device and One Ratio of Note 21

Table 3-2: NPN and PNP BJT Size Ratio for Each Device Compared an Average Small NPN or PNP BJT (1-4). 22

Table 3-3: TID to Proton Fluence Conversion 23

Introduction

When bipolar junction transistors (BJTs) are exposed to neutrons, the current gain degrades due to displacement damage in the semiconductor material [1]. Traditionally a "bag test" is used to simulate the neutron environment. In this kind of test, the parts are shipped to a neutron facility where they are placed in an unbiased state next to a nuclear reactor and irradiated to a specified neutron fluence. This kind of testing can be cumbersome. After neutron irradiation, parts can begin annealing immediately, meaning that measurements must be taken promptly. However, the parts may be hot after irradiation, causing timely measurements to be difficult. Furthermore, there are fewer neutron sources available than formerly [2]. One way around these issues is to introduce displacement damage using proton irradiation. However, interpreting the results of proton irradiation is more complicated because protons are charged particles and cause ionization damage [3].

Neutron and proton irradiation of a bipolar junction transistor, or BJT, lowers the current gain, and is most pronounced at low emitter-base bias levels due to increased base current [4], [5]. Irradiation causes increased bulk recombination due to lattice displacement that creates traps in the bulk silicon. As a result, the minority carrier lifetime is decreased, the majority carrier density is changed, and the carrier mobility is reduced. When a neutron or other particle interacts with the silicon lattice, it knocks a particle from its position in the crystal and creates a vacancy. The atom then settles in an interstitial location some distance away from the site of impact, creating a Frenkel pair. Often times, there is more than one particle that is displaced, showing up as a cluster of defects. Typically, displacement damage is measured and simulated through non-ionizing energy loss, or NIEL, which is proportional to displacement damage [3], [6], [7].

With the use of protons, it is also important to discuss the effects of total ionizing dose, or TID, because a proton is a charged particle. The main effect of TID is the creation of electron-hole pairs in both silicon and silicon dioxide. Ionizing radiation causes surface recombination, resulting in increased base current and reduced current gain [3]. In SiO_2, the creation of electron-hole pairs results in holes trapped in the oxide. The most probable location for charge trapping is near the Si/SiO_2 interface. The holes may also liberate hydrogen in the oxide that will transport to the interface and react to create interface traps [4], [5].

Both displacement and ionization damage effects are manifested as decreases in current gain, or β, where gain is the ratio of collector current to base current, or I_c/I_b. The decrease in gain is due primarily to the increase in base current described above. The amount of device degradation due to irradiation has also been shown to depend on both device geometry and doping [3]–[5], [8]–[12]. Research has shown that 10 keV X-rays can be used to simulate the effects of ionization energy of protons. However, to get an accurate measure of displacement damage caused by protons, it is necessary to correct for proton charge yield compared to 10 keV X-rays [13].

The mechanisms for both displacement damage and ionizing damage are discussed (Chapter 1) followed by an analysis of proton irradiation and displacement and ionization correlation (Chapter 2). This work describes the results of irradiating NPN and PNP BJTs of different sizes to examine the effects of protons on current gain. The devices were irradiated with 4 MeV protons and 10 keV X-rays. The results show that protons can provide a useful first-order screen for sensitivity to displacement damage (Chapter 3).

Chapter 1

1.0 Review of Mechanisms

1.1 Displacement Damage

When energetic particles interact with silicon or other semiconductors, they lose their energy to both ionizing and non-ionizing processes. Displacement damage is the result of a non-ionizing process where an atom is displaced from its lattice position. When this happens, it creates a vacancy and an interstitial, or a Frenkel pair. This is caused by a mechanism where a large amount of energy is transferred from a neutron or other particle to a single silicon atom. This atom is a primary knock-on atom, or PKA. The PKA can then dislodge other atoms creating a region with multiple defects [7]. The range of defects is shown in Figure 1-1 for simulated protons. For energies under 2 keV, there are only point defects, but as the energies get higher there are cascades, or single defect clusters, and then sub cascades, or multiple defect clusters [14]. The displacement of atoms introduces new energy levels in the band gap that act as recombination centers. This alters the electrical properties of semiconductors by reducing carrier lifetime [3], [7].

NIEL can be calculated from first principles based on differential cross sections and is the energy introduced by elastic nuclear and Coulombic reactions, as well as nuclear inelastic reactions. These interactions introduce displacement damage and phonons. NIEL can be described for any type of particle using the following expression [7]:

$$NIEL = \frac{N}{A}\,[\sigma_e T_e + \sigma_i T_i]$$

In this expression, σ_e and σ_i are elastic and inelastic cross sections, respectively, and T_e and T_i are elastic and inelastic effective average recoil energies corrected for ionization

loss. *N* is Avogadro's number and *A* is the gram atomic weight of the target material. The units of NIEL are MeV-cm^2/g. Research performed since the concept of NIEL was developed has shown that for multiple device types, to first order, there is a linear relationship between device degradation due to particles and NIEL [7].

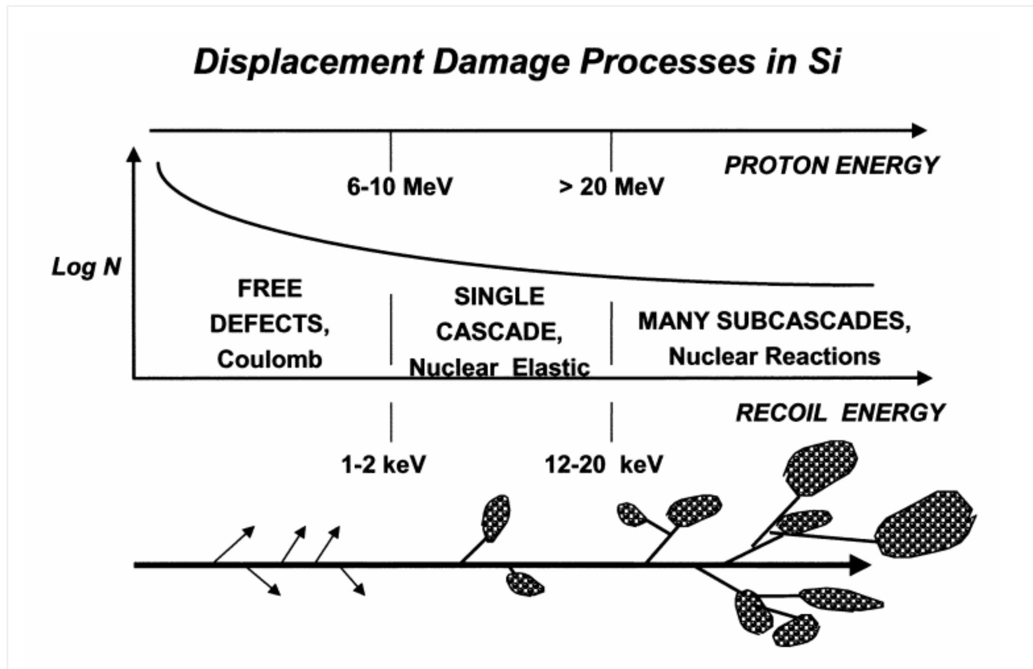

Figure 1-1: Spatial distribution of initial defect configuration due to primary knock on atom for proton irradiation, after [14].

Work by Messenger and Spratt in 1958 derived a linear relationship to describe the relationship between particle fluence and current gain [15]:

$$\frac{1}{\beta(\Phi)} = \frac{1}{\beta_{pre}} + K(E)\Phi$$

where *K(E)* is the particle and energy dependent displacement damage factor and Φ is the particle fluence. A linear relationship between parameters such as reciprocal current gain or minority carrier lifetime can be seen when transistors are irradiated with incremental

fluences [7]. The rate of this linear relationship can change with different particles and different particle energies as shown in Figure 1-2 [16]. The damage factor for a specific energy particle on a device is then defined as the linear rate of change, or slope [3], [7]. For a BJT, it represents changes in the recombination rate in the different regions of the transistor [7].

Furthermore, a damage factor at increasing collector current or emitter-base voltage can be calculated to show how bias affects radiation response. It also can be used to compare radiation response between different types of ions. Using this analysis, Summers *et al.* showed that even as the damage factor changes with biasing, the ratio of a particle's damage factor to neutron damage factor stays constant as shown in Figure 1-3 [16].

Knowing the damage factor between a given particle and neutrons allows the use of monoenergetic particles to predict device response in radiation environments and relate the damage from one particle to another with a different energy. From this, radiation response can be predicted using calculations of the amount of energy transferred to the primary knock on atoms. A function to describe nonionizing energy loss, or NIEL, was developed to describe this relationship [3], [7], [16]. Research by Burke *et al.* postulated a more thorough set of calculations for NIEL that could both predict energy dependence of the device damage factor and correlate degradation due to different particles [17]. This research was confirmed by experimental data from Summers *et al.* and Dale *et al.* [16], [18] Later it was expanded on by Messenger *et al* and Jun *et al*. to facilitate more accurate results [19], [20]. This will be discussed in Chapter 2 with a focus on protons.

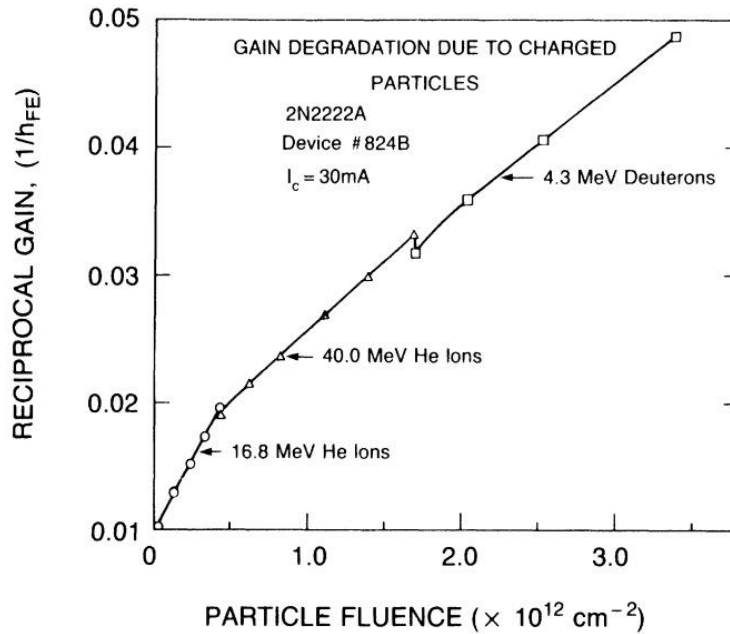

Figure 1-2: Reciprocal gain vs. fluence for sequential irradiation of the same 2N2222A NPN transistor with 16.8 MeV and 40.0 MeV helium ions and 4.3 MeV deuterons, after [16]. The slope, or damage factor changes for each type of ion.

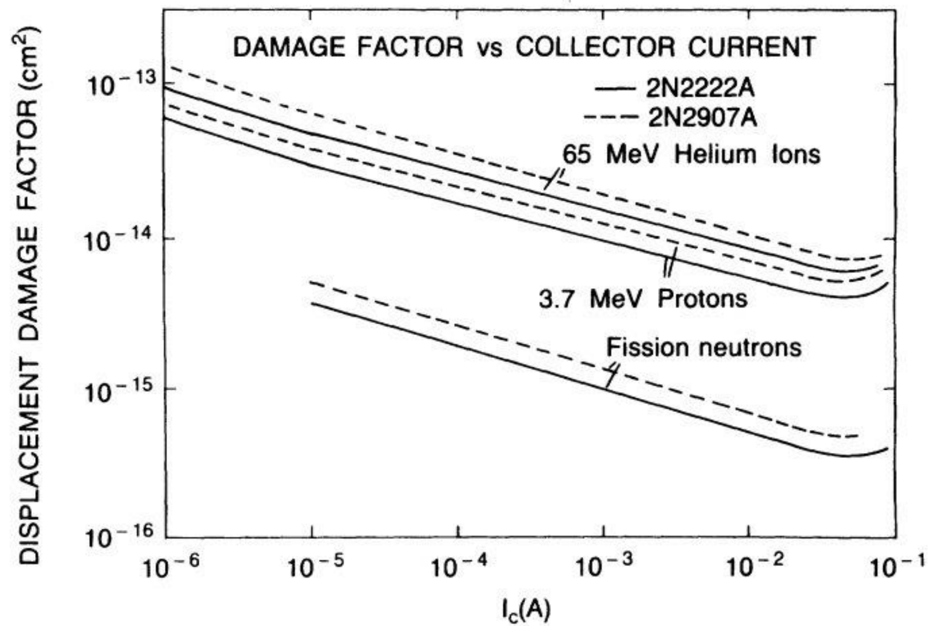

Figure 1-3: Displacement damage factor as a function of collector current for an NPN and PNP transistor with neutrons, 65 MeV helium ions, and 3.7 MeV protons, after [16].

1.1.1 Effects in BJTs

The main effects of radiation damage on BJT's are increased recombination of electron-hole pairs and compensation of donors or acceptors by radiation-induced centers. In electron-hole pair recombination, a free carrier is captured by a defect center, followed by the capture of the oppositely charged particle, thus removing carriers. The amount of defect centers depends on the amount of radiation damage. As more defect centers are created, the minority carrier lifetime decreases, causing gain degradation. As the carrier lifetime decreases, the base current increases [3], [7]. Another less prevalent effect is the compensation of dopants. Radiation-induced defects that act as donors or acceptors compensate some of the minority carriers. For example, in n-type material, radiation-induced acceptors will compensate some of the donors. In BJT's, this is shown as in increase in resistance due to the removal of carriers [7].

In an experiment by H.S. Hajghassem *et al*., multiple NPN BJT's were irradiated with 1 MeV equivalent neutrons with fluences ranging from 1×10^{12} to 1×10^{14} cm^{-2}. Figure 1-4 shows a Gummel plot with pre and post irradiation results for the 2N2222 BJT exposed to a neutron fluence of 1×10^{14} cm^{-2}. The collector currents remains relatively unchanged while there is a noticeable increase in the base current. At low voltages, the post-irradiation current is more than one order of magnitude higher than the pre-irradiation value. These effects are due to radiation-induced surface recombination, emitter-base space charge recombination and emitter-base current channels [21]. This shows the recombination rate increases throughout the depletion region due to displacement damage rather than just at the Si/SiO_2 interface as in total ionizing dose [4], [5].

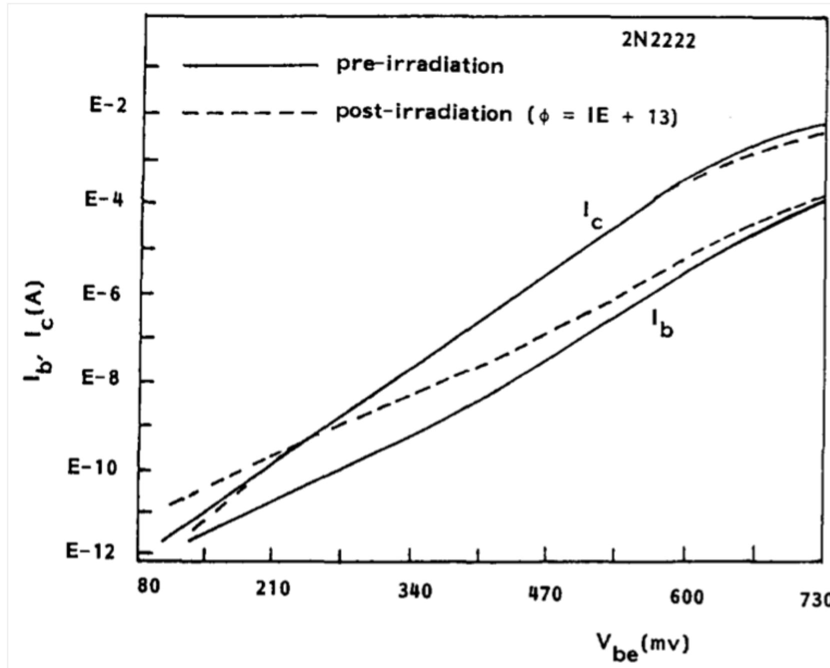

Figure 1-4: Gummel plot for a 2N2222 BJT pre and post neutron irradiation, after [21].

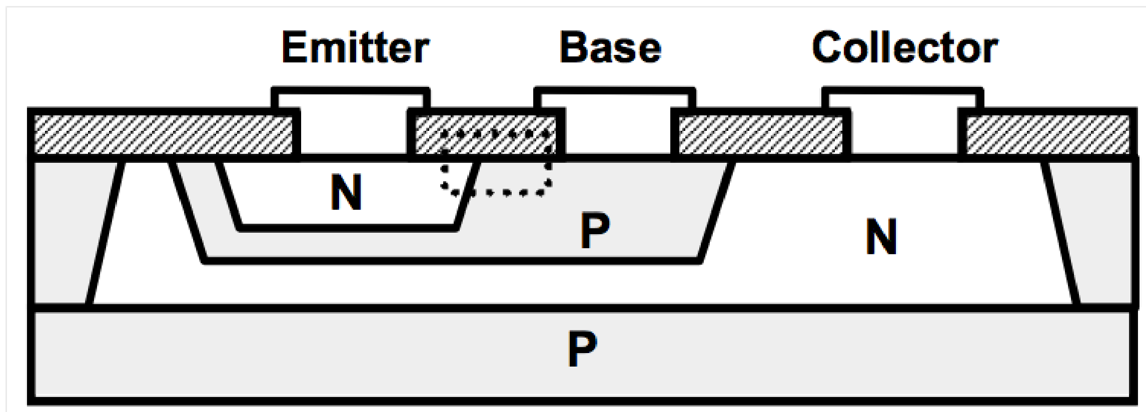

Figure 1-5: Cross section of a typical NPN BJT. The dashed line represents the area most sensitive to ionizing radiation, after [4].

1.2 Total Ionizing Dose

Ionizing damage can be caused by many sources including protons, electrons, and photons [3], [4]. The most prevalent type of degradation due to ionizing radiation in BJTs is the reduction of current gain due to excess base current [3]–[5], [8], [11], [12], [22]–[24]. Before irradiation, base current is dominated by back injection from the base to the emitter [25]. After a BJT is exposed to ionizing radiation, the base current is dominated by recombination in the emitter-base depletion region [4], [5].

The increase of base current is mainly caused by a combination of interface traps and trapped positive oxide charge near the emitter-base depletion region. Figure 1-5 shows the cross section of a typical NPN BJT with the emitter-base region outlined with a dotted line. The oxide charge increases surface potential changes the area of the depletion at the surface of the device while the interface states increase surface recombination velocity [4], [5], [11], [12], [22], [23]. In certain circumstances, it has been shown that gain can also decrease due to a reduction in collector current [8], [26].

Figure 1-6 shows normalized current gain for increasing values of Total Ionizing Dose. The BJT's in this example were NPN polysilicon emitter bipolar transistors fabricated using a BiCMOS process. The transistors were irradiated with 10 keV X-rays at a dose rate of 1.7 krad(SiO_2). The current gain degradation tends to saturate at larger doses. In this irradiation, the collector current remains constant while the base current increases. [12], [27].

In Figure 1-7, the ideality factor for all of these currents is close to 2. In a BJT, the relationship between current and voltage can be described by the equation:

$$I = I_0 \, e^{\frac{qV}{N_e kT}}$$

where I_0 is a generalized saturation current and N_e is called the ideality factor. When this equation is plotted as the log of current vs. voltage, the result is a straight line where n is related to the slope. Ideally, the value of N_e is 1. When n = p, the ideality factor is closer to 2 because this is the location of maximum recombination. Currents that are produced by radiation-induced recombination usually have an ideality factor between 1 and 2 [4], [5]. Oxide charge far from the emitter-base junction is generally what determines the ideality factor. It is interesting to note that the increases in total dose do not affect the excess base current in a meaningful way once $N_e = 2$ [12].

1.2.1 NPN BJT Mechanisms

Positive charge increases the surface potential in the intrinsic base causing an increase in the surface recombination velocity and the spreading of the emitter-base depletion region [4], [12]. This means that the recombination rate increase appears near the Si/SiO_2 interface because of the interface traps serving as recombination centers [22]. Eventually the number of electrons and holes at the surface will become equal meaning that the recombination rate is at a maximum. As more oxide charge accumulates, the area for maximum recombination will move subsurface. The amount of excess base current will increase super-linearly until the recombination becomes subsurface. Then, the amount of excess base current will saturate. This saturation was shown to occur independently of dose rate or irradiation bias [4], [5], [9], [27].

The increase of the SRV is proportional to the density of recombination centers at the interface covering the emitter-base junction. The oxide charge is positive, meaning that the depletion region will spread into the p side of the junction [4], [5]. Increased recombination

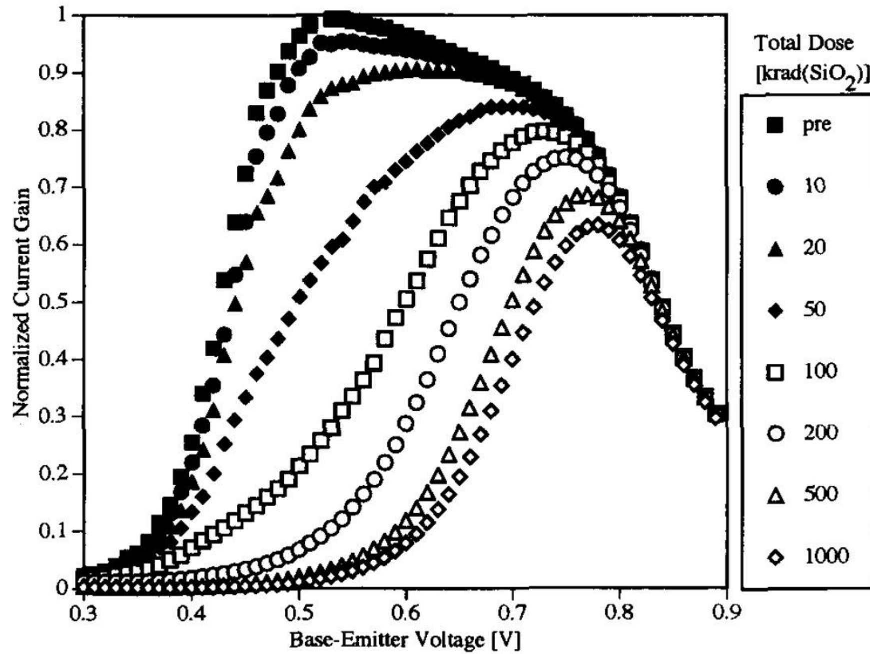

Figure 1-6: Normalized current gain versus base-emitter voltage for increasing levels of total ionizing dose, after [12].

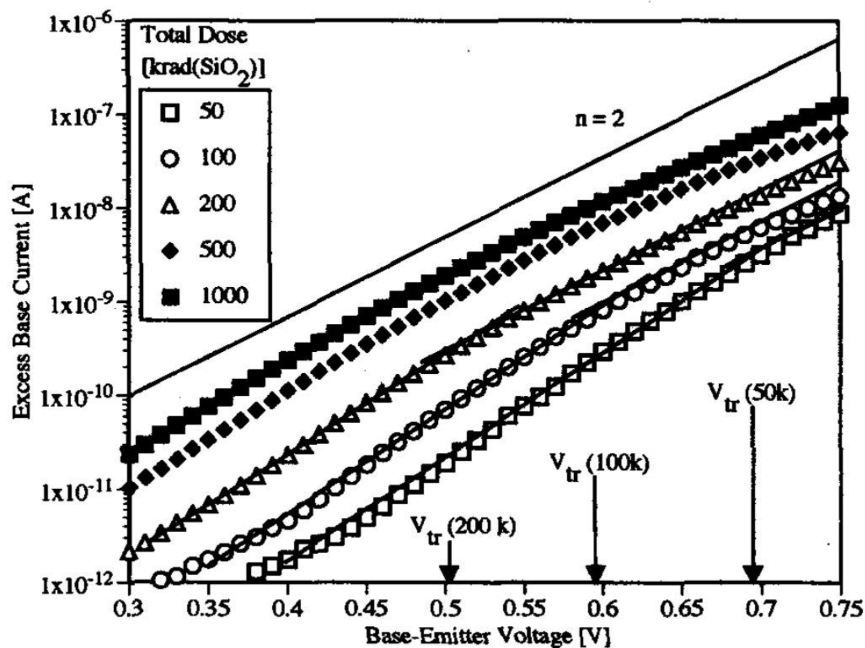

Figure 1-7: Excess base current versus base-emitter voltage for various levels of total ionizing dose with an ideality factor of 2 super imposed for comparison, after [12].

occurs around the edge of the emitter. The amount of excess base current is related to the ratio of emitter area to emitter-base interface [11].

In research by Nowlin *et al.* the post radiation current gain of the NPN transistors tested was about 40% of the original gain. The oxide charge was shown to have a large effect over p-type material, or the base region for an NPN BJT. The lower doping level in this region facilitates this effect as the depletion region expands more into the base and increases recombination with the minority electrons [22].

1.2.2 PNP BJT Mechanisms

Vertical PNP BJTs (VPNP), similar to the devices in this research, are more radiation tolerant than other transistor structures. Interface traps at the Si/SiO_2 increase the SRV causing excess base current. However, positive oxide charge forces the holes in the n-type base below the surface causing an imbalance of electrons and holes and reducing the width of the emitter-base depletion region, as shown in Figure 1-8. It also depletes the p-type emitter, but only has a small effect due to the high p-type doping. This causes a reduction in surface recombination. Consequently, these two mechanisms counteract each other. The effect is also smaller in a PNP BJT due to the emitter region being more highly doped p-type than the p-type base of an NPN BJT [4], [5]. Furthermore, the vertical current flow reduces the area of depletion region that is adjacent to oxide [9]. By comparison, in a lateral PNP (LPNP) BJT as shown in Figure 1-9, the dominant gain degradation mechanism is recombination centers at the Si/SiO_2 interface resulting in increased SRV. Since the current flow is directly under the oxide, this has a large effect [4], [5].

A comparison of these two transistor structures and a substrate PNP (SPNP) BJT was done by Schmidt *et al.* In this work, the total ionizing dose required to degrade the LPNP

BJT to ½ of its normalized gain was 50 times less than the total dose required to get the same degradation in a VPNP BJT. The SPNP BJT required 20 times less total dose than the VPNP BJT to reach ½ of its normalized gain. The VPNP BJT shows the least amount of degradation. Figure 1-10 shows the normalized current gain for each transistor type as a function of total dose and Figure 1-11 shows a pre-radiation gain plotted vs. emitter-base voltage against post-radiation results from each of the three transistor types [9].

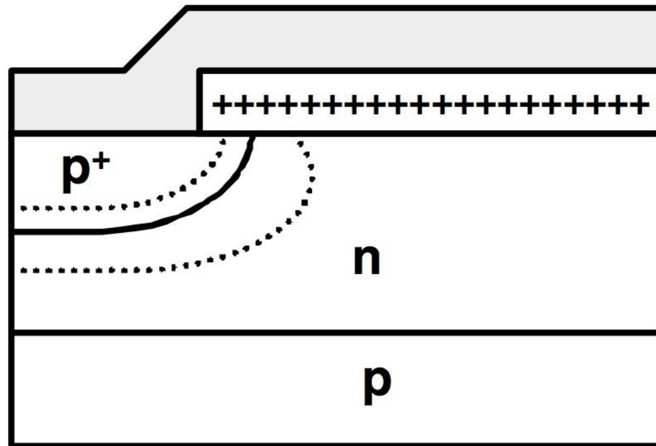

Figure 1-8: A diagram of a generic vertical PNP transistor showing how the depletion region narrows in the n-type base due to positive oxide charge, after [4].

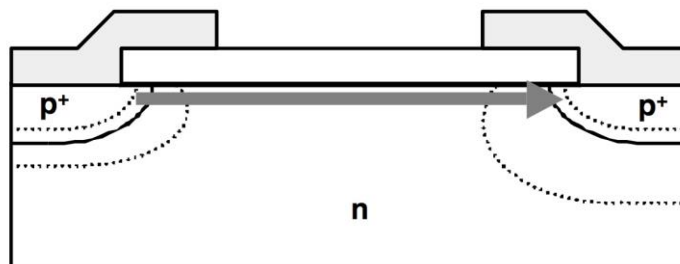

Figure 1-9: A diagram of a lateral PNP transistor showing current flow under oxide, after [4].

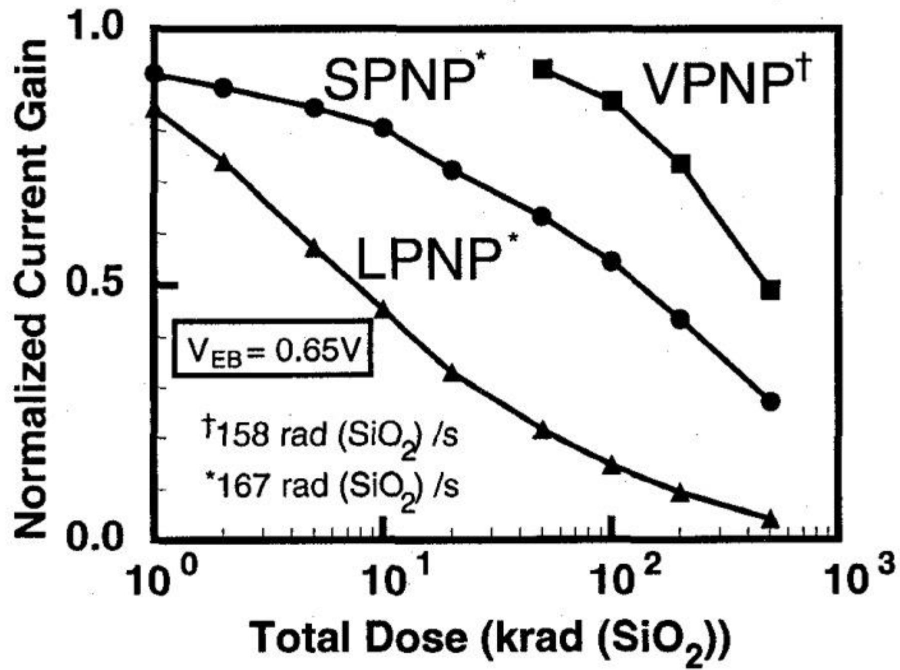

Figure 1-10: Normalized current gain vs. total dose from lateral (LPNP), substrate (SPNP), and vertical (VPNP) BJTs [9].

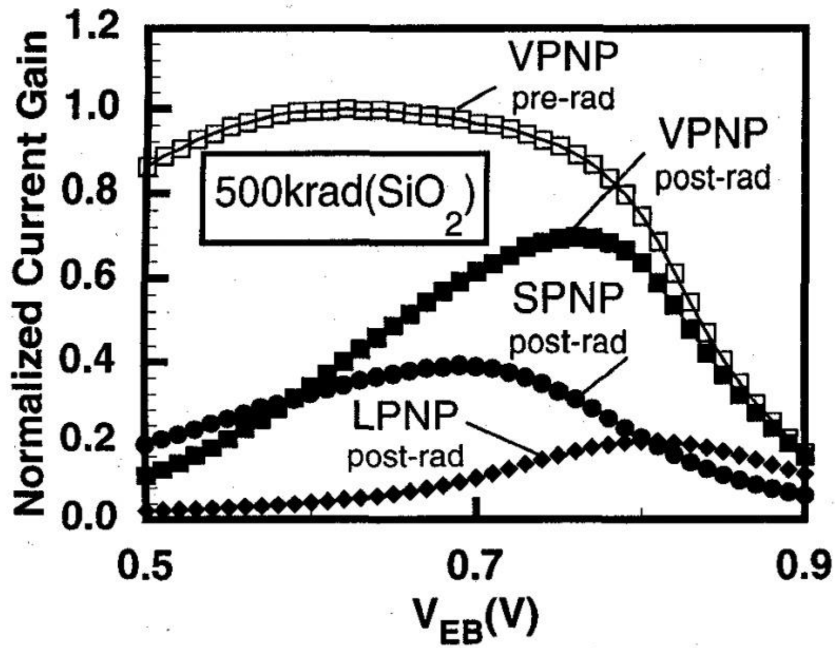

Figure 1-11: Normalized current gain vs. emitter-base voltage from lateral (LPNP), substrate (SPNP), and vertical (VPNP) BJTs at a dose of 500 krad(SiO_2) [9].

Chapter 2

2.0 Effects of Proton Irradiation

Proton irradiation causes increased bulk recombination due to displacement damage and surface recombination due to ionization damage. Initially, studies used separate irradiations to simulate the two types of damage from one another, but later studies have shown that bipolar technologies actually exhibit a different response to the combination of effects [28]–[30]. While displacement damage caused by protons scaled linearly with NIEL, ionization induced oxide charge causes a non-linear response [2], [16], [18], [28], [29].

2.1 Correlating Protons for Displacement Damage

Summers et al. showed how particle-induced displacement damage could be correlated. For these experiments, BJTs were subjected to a total dose of 1500 krad(Si) to saturate ionization damage before being exposed to protons for displacement damage studies [16]. These results were explained above in Chapter 1.1.1. While giving an excellent correlation of protons to neutrons for displacement damage (as shown in Figure 2-1), the scope of that research did not include the effects of proton ionization [16]. Similar conclusions were made by Pease *et al.* and Raymond *et al.* [30], [31]. Further work by Summers *et al.* claimed that there is a direct proportionality between proton damage coefficients and NIEL that appears to hold for all parameters on any given device. Therefore, all that would be needed for a calculation would be a differential proton flux, measurements made at 1 proton energy, and a calculated value of NIEL [32]. Later work by Jun *et al.* found even more accurate NIEL values for protons by taking into account Coulomb scattering for protons under 10 MeV [19].

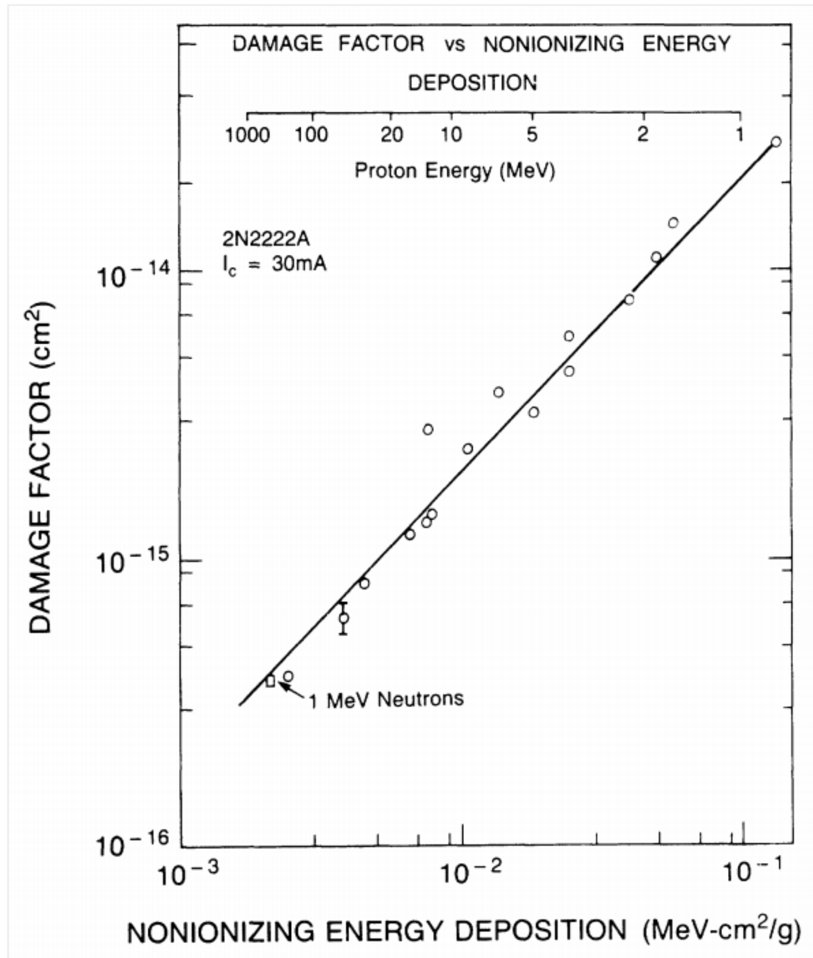

Figure 2-1: Linear relationship between measured damage factors for 2N2222A transistors and calculated NIEL for protons. Corresponding proton energy is shown at the top [16].

2.2 NIEL for Protons

The value of NIEL for protons has been calculated with a variety of methods as discussed above. Table 2-1 shows a comparison of values for 4 MeV protons as calculated by Summers *et al.*, Jun *et al.*, and by MRED [19], [32]. As can be seen, Summers *et al.* and Jun *et al.* agree very closely with Jun's number being lower as it accounts for the Coulomb scattering of the protons [19].

Table 2-1: NIEL Values for 4 MeV protons Calculated by Different Methods

Method	**NIEL (MeV cm^2/g)**
Summers *et al.*	0.0192
Jun *et al.*	0.0189
MRED	0.0142

2.3 Effects of Simultaneous Displacement and Ionization Damage

Work by Rax *et al.* investigated the effects of proton irradiation on bipolar devices. Instead of focusing solely on displacement damage caused by protons, it also looked at ionization effects. Parts irradiated with both protons and gamma rays showed significantly more damage from protons at identical total dose levels due to displacement damage. In comparing the effects of ionization, it was found that gamma rays caused more ionizing damage the protons. Therefore, subtracting gamma ray damage from proton damage underestimated the amount of displacement. It was also found that the relative amount of displacement and ionization damage depends on the energy of the protons [33]. Furthermore, it was shown that device geometry could also impact its sensitivity [33], [34].

Research conducted by Barnaby *et al*. in 2001 and 2002 compared the effects of proton radiation in commercial off the shelf, or COTS, parts with the effects of neutron and X-ray radiation. While parts qualifying has traditionally been done assuming that displacement damage and total ionizing dose are separate, this research found that by taking separate X-ray and neutron irradiation and combining the results to simulate protons over-estimated the amount of damage [28], [30]. Figure 2-2 shows this relationship [28].

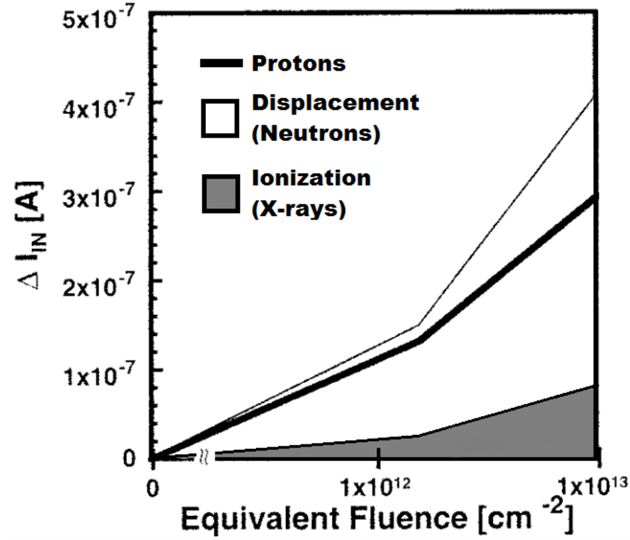

Figure 2-2: Change in LM124 bias current versus equivalent fluence for X-ray (ionization), neutron (displacement), and proton irradiations, after [28].

Current degradation cannot be modeled as a sum of X-ray and neutron interaction because the sum of degradation does not account for the effects of oxide charge on carrier recombination in the semiconductor bulk in BJTs [28]. As discussed above, oxide, interfacial, and bulk defects introduced by protons increase carrier recombination in the emitter base depletion region and the neutral base [23], [35]. The interface traps increase the surface recombination (R_S) and the bulk traps increase bulk recombination (R_B). The relationship of excess base current to R_S and R_B is:

$$\Delta I_B \ \alpha \int_A R_S(\vec{r})\, r dr + 2\int_V R_B(\vec{r})\, r^2 dr$$

The oxide charge suppresses R_B in PNP BJTs by increasing the major carriers at the base surface and enhances it in NPN BJTs by lowering the majority carrier density [29]. Note that the surface recombination depends on the size of the emitter-base surface and the bulk recombination depends on the size of the emitter-base volume [28]. From this data, Barnaby

et al. created a model that can determine what portion of damage is due to a variety of combinations of X-rays, neutrons, and protons based on the depth and doping of the base. Of interest to this research is the proportion for X-rays to protons as shown in Figure 2-3.

Research has also been done to compare the ionization effects of 10 keV X-rays and 1.25 MeV Cobalt 60 with a range of proton energies [13]. The results of this work showed the ionization damage caused by protons was similar to the damage caused by 10 keV X-rays. This is due to the similarities in stopping powers and the similar charge yield from secondary electrons of 10 keV X-rays and lower energy protons. However, the range of protons previously tested have mass stopping powers that were both higher and lower than the secondary electrons from 10 keV X-rays [13], [36]. The difference in mass stopping power has an effect on the charge yield of protons and makes a correction factor necessary to calculate the exact amount of ionization caused by protons [13]. The application of a charge yield correction relating to the 4 MeV protons used in this work is explained in Section 3.3.

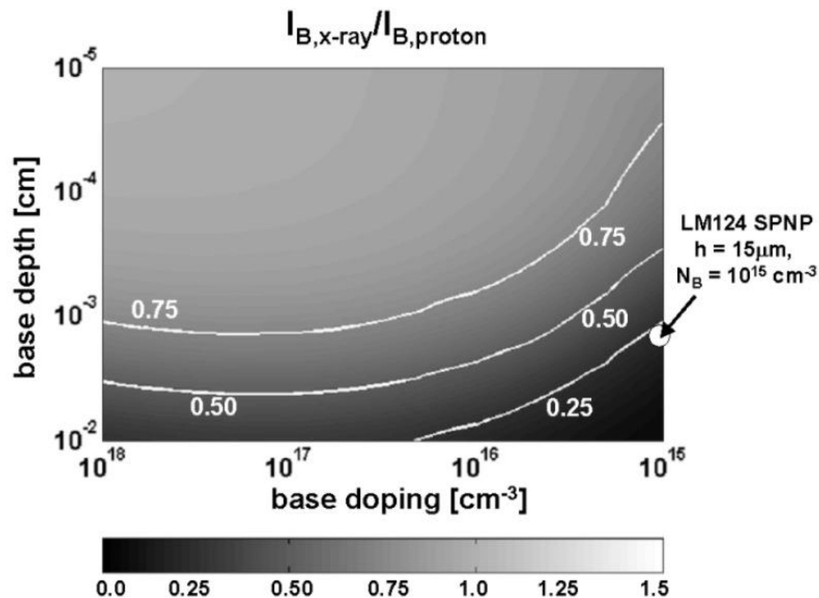

Figure 2-3: Analytically calculated ratio of X-ray to proton radiation response based on depth and doping of the device base, after [29].

Chapter 3

3.0 Experimental Results

3.1 Experimental Details

The devices used in this study were BJTs manufactured using Texas Instruments' BiCOM 1.5 process. They were fabricated on bonded silicon-on-insulator substrates using deep trench isolation. Figure 3-1 shows a cross section of both NPN and PNP BJTs from an Intersil PR40 process similar to BiCOM 1.5 [37].

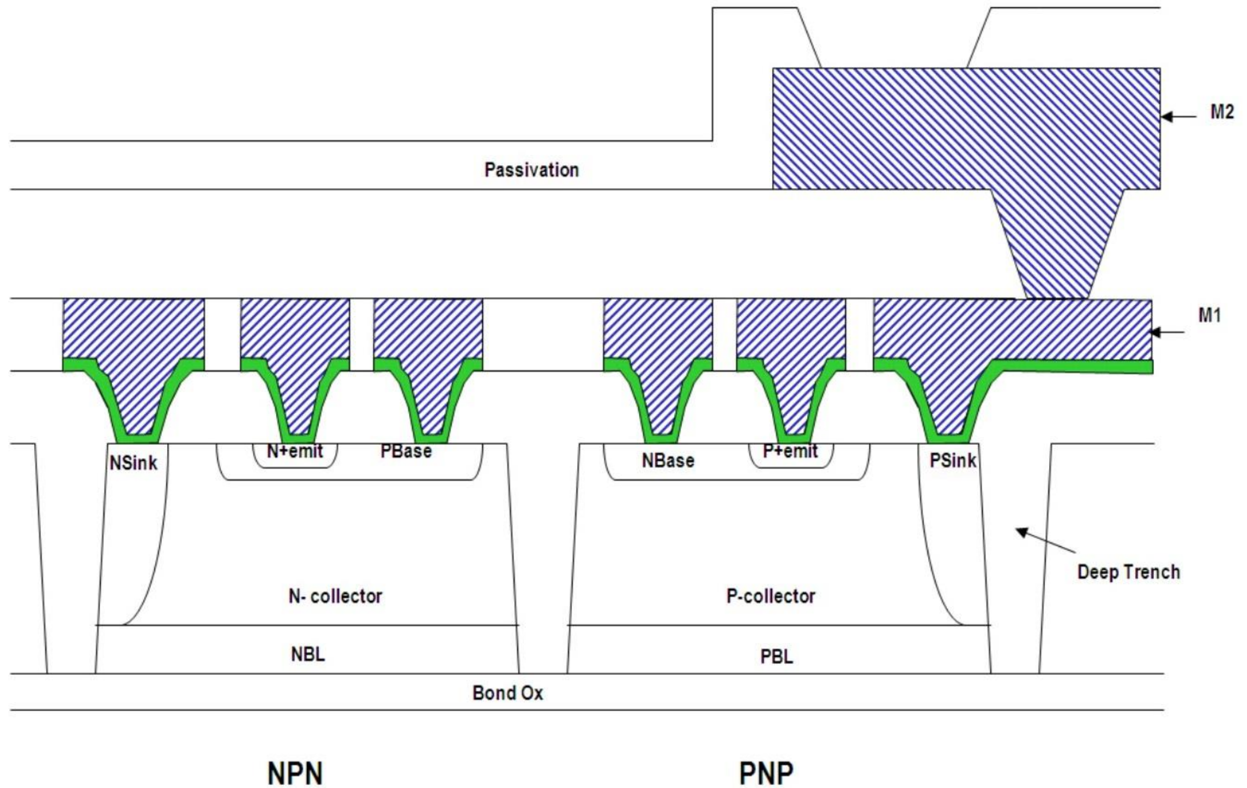

Figure 3-1: Cross section of BJTs in Intersil's BiCMOS process [37].

In this study, the test structures were fabricated with 12 NPN BJTs and 11 PNP BJTs of varying sizes. The chips were packaged in 40-pin DIPs with the pins connected to either

the NPN BJTs or the PNP BJTs such that each terminal on a transistor had its own pin. Due to how the chips were bonded and some test setup issues, 11 NPN BJTs and 9 PNP BJTs were used from each chip. To account for part-to-part variability, two NPN BJT and two PNP BJT test structures were irradiated with protons and two of each were irradiated with X-rays. This accounted for 8 total parts, or 44 NPN BJTs and 36 PNP BJTs.

While the exact device dimensions are not known, their relative size compared to other transistors on the chip could be calculated. An image of the device layout was expanded to relatively large size; for each device, a measurement of how many pixels tall and wide was taken to get a relative size. NPN and PNP BJT device sizes were compared and are shown as a ratio of each other in Table 3-1. As a result, certain other devices were compared to show they are also of similar size.

Table 3-1: PNP BJT to NPN BJT Ratio for Each Device and One Ratio of Note

Device	**Ratio (P/N)**
1	1.10
2	0.93
3	1.01
4	0.92
5	0.92
6	0.97
7	1.04
8	1.28
9	1.31
10	N/A
11	N/A
12	N/A
Other Device Ratio of Note	
PNP 8/NPN 9	1.00

It was found that devices 1-4 for both NPN BJTs and PNP BJTs were of similar size. Using the average of the area of NPN BJTs 1-4 and PNP BJTs 1-4 respectively as a standard,

the relative size of all of the devices were calculated. These numbers are shown in Table 3-2. The largest device for this experiment was 9.51 times the size of the smaller devices.

Table 3-2: NPN and PNP BJT Size Ratio for Each Device Compared an Average Small NPN or PNP BJT (1-4).

Device	NPN BJT	PNP BJT
1	0.88	0.99
2	1.04	0.98
3	0.99	1.01
4	1.09	1.02
5	1.33	1.24
6	1.57	1.55
7	2.12	2.24
8	2.42	3.16
9	3.11	4.13
10	N/A	N/A
11	6.11	N/A
12	9.51	N/A

The chips were placed in a 40-pin zero insertion force DIP that was connected via a 40-conductor ribbon cable with 22 AWG wires for the conductors to a multiplexor on a Keithley 3706-S system switch. The output of the mux was connected to a HP 4156B with one channel for collector, emitter, and base. The substrate of the device was connected to the hard ground. The mux and 4156B were controlled via GPIB from a computer running code to sweep one transistor at a time on a device.

Using this setup 11 NPN BJTs or 9 PNP BJTs were irradiated at one time. 4 MeV protons from the pelletron at Vanderbilt University were used and 10 keV X-rays were used from an ARACOR 4100 also at Vanderbilt University. The parts were irradiated according to a total ionizing dose measured in krad(Si). For the protons, an equivalent fluence was calculated based on a simulation using the Monte Carlo Radiative Energy Deposition (MRED) software based on Geant4. This calculated that each 4 MeV proton

particle causes 1.16 x 10^{-9} krad(Si). Using this value, it is possible to equate total ionizing dose to particle fluence. Table 3-3 shows the corresponding total dose and fluence amounts used in this experiment.

Table 3-3: TID to Proton Fluence Conversion

TID (krad [Si])	Fluence (cm^{-2})
50	4.31 x 10^{10}
100	8.62 x 10^{10}
300	2.59 x 10^{11}
500	4.31 x 10^{11}
700	6.03 x 10^{11}
1000	8.62 x 10^{11}
1500	1.29 x 10^{12}

A calculation using an LET value from SRIM using the equation:

$$TID[rad(Si)] = LET[MeV cm^2/g] \times \Phi[cm^{-2}] \times 1.6 \cdot 10^{-8}[100ergs/MeV]$$

produced similar values within 5% of the MRED calculations.

After the parts were irradiated, annealing measurements were taken. These measurements were t_{anneal}*0.33, t_{anneal}, 24 hours, and 1 week. For TID, t_{anneal} = 26.5 minutes and for protons t_{anneal} = ~10 minutes.

3.2 Comparison of Proton and X-ray Data

The data collected for each device were current and voltage values for the emitter, base, and collector. Figure 3-2 is a Gummel plot for a single PNP BJT irradiated with protons. Only the collector current from the prerad measurement is plotted compared to the base currents for prerad through the 1500 krad(Si) equivalent fluence. The increasing base current due to proton damage can clearly be seen. Similarly, Figure 3-3 is a Gummel plot for a single PNP BJT irradiated with X-rays. Here, there appears to be less of an increase in base

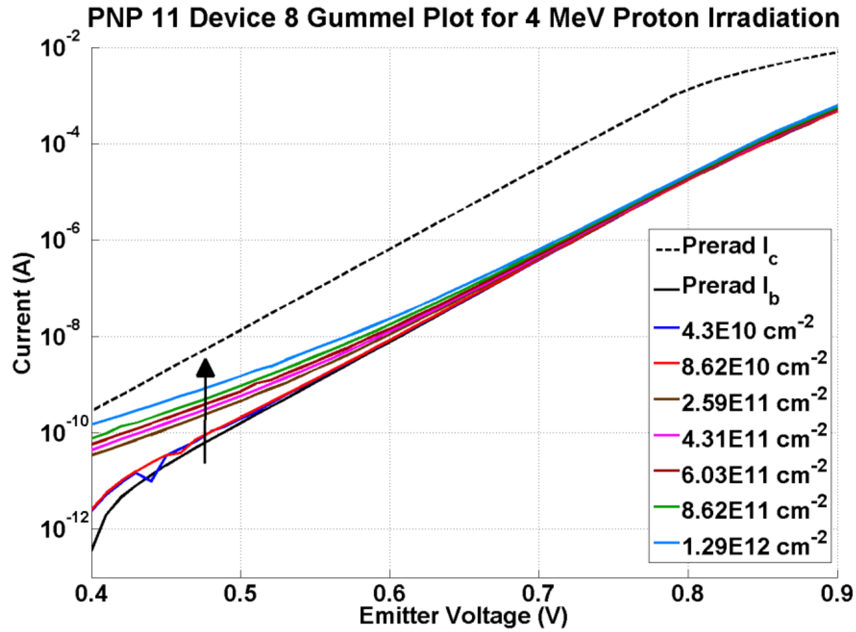

Figure 3-2: Gummel plot of a PNP device irradiated with 4 MeV protons. Note the increasing current base current as the radiation increases.

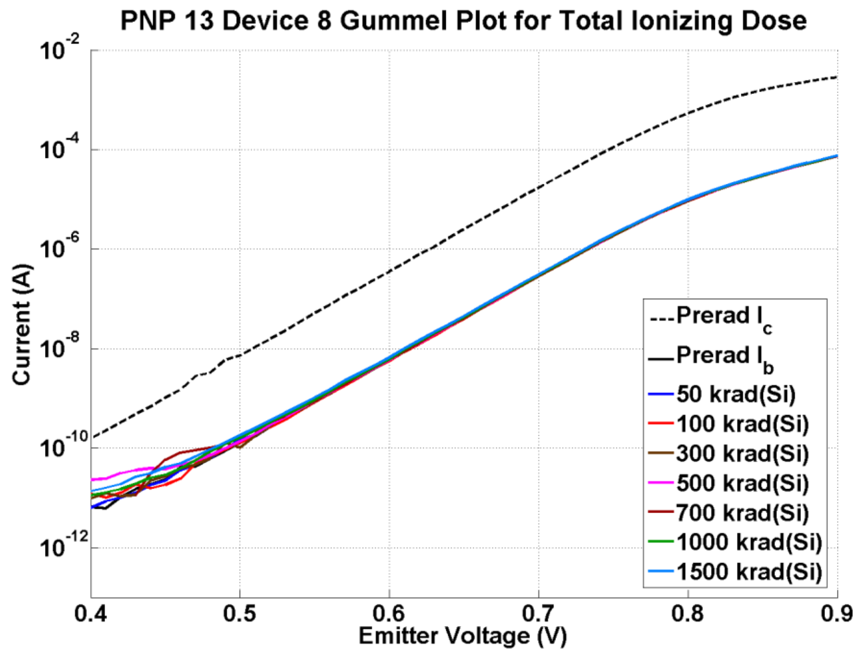

Figure 3-3: Gummel plot of a PNP device irradiated with 10 keV X-rays. Note the much smaller magnitude of excess base current.

current due to the X-rays. On both of these plots there are areas where the current was too low for the 4156B to register. The beta plot for PNP 11 Device 8, Figure 3-4, shows an infinite gain until the current measurement was high enough to register. From 0.5V to 0.9V there is a reliable and clean measurement that clearly shows gain degradation due to proton damage.

Damage Factor (k) is calculated as the slope of reciprocal gain at the proton fluence levels. It is a useful way to characterize the change due to radiation in BJTs because gain is described as I_C/I_B. Taking the reciprocal of this number gives the base current as the numerator. Since the collector current changed a negligible amount due to radiation, reciprocal gain shows the change in base current while being able to ignore temperature effects. The damage factor then describes the change in base current due to different particle fluences.

Figure 3-5 is a plot of the reciprocal gain of 4 PNP devices of the same size. The X-ray values are plotted according to their equivalent proton fluence, as shown in Table 3-3, for easy comparison. The lines plotted show a linear response to both X-ray and proton irradiation. From this plot, it appears that PNP 13 (exposed to X-rays) had a much lower gain to start with. This lower gain actually appears for all devices on PNP 13 and can probably be attributed to process variation. Figure 3-6 shows a corresponding reciprocal gain plot for a similarly sized set of NPN BJTs. Again, there is a linear response. The slopes for proton irradiation appear to be very similar to the PNP devices while the slope for X-ray irradiation appears to be higher than the PNP devices. These slopes are considered to be the damage factor for their respective devices at a bias of 0.6 V.

Figure 3-7 and Figure 3-8 show k for each of the PNP and NPN BJTs at their respective size ratio at an emitter-base voltage of 0.6 V. From this it can be seen that there are no definitive effects relating radiation damage to device size. While there are differences in the k values, they are probably due to process variation. The biggest indicator of this would be that the devices with a size ratio of 1 appear to have just as much variation among themselves compared to the rest of the devices. However, more work needs to be done to verify this claim.

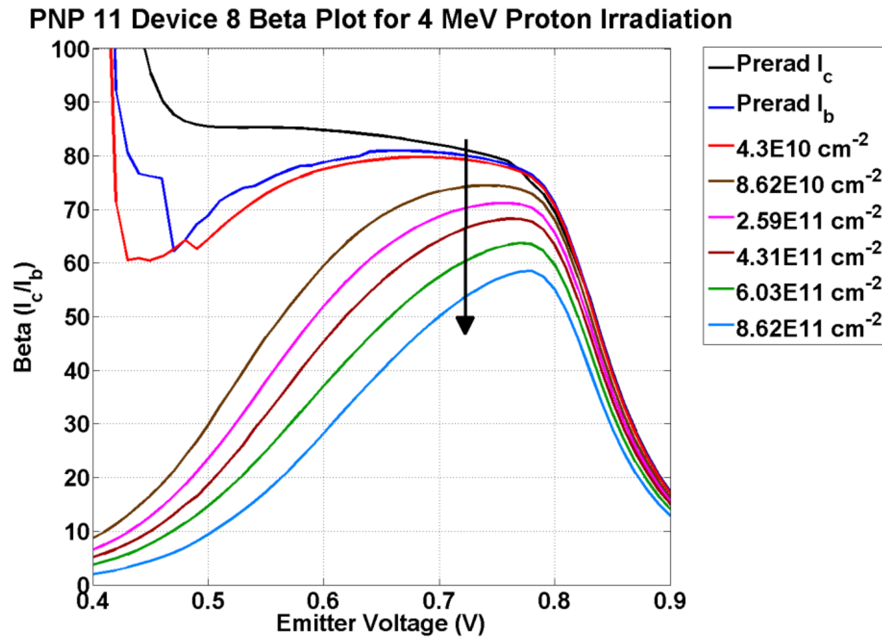

Figure 3-4: Beta plot of a PNP device. Note the decreasing gain as the radiation increases.

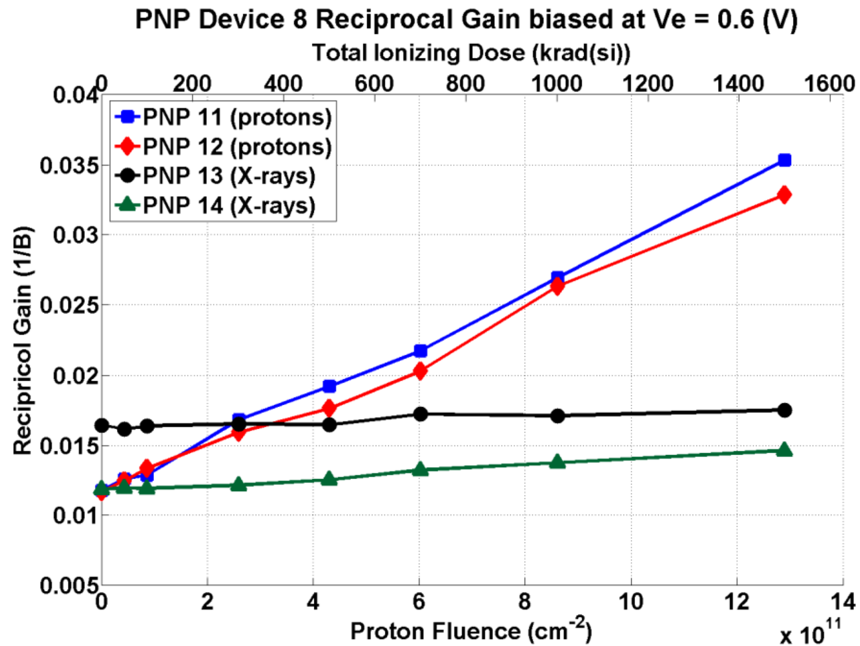

Figure 3-5: Reciprocal gain plot of four PNP devices the same size. There is a linear increase for both the proton and X-ray irradiated parts. The slope of these lines is the damage factor at this bias.

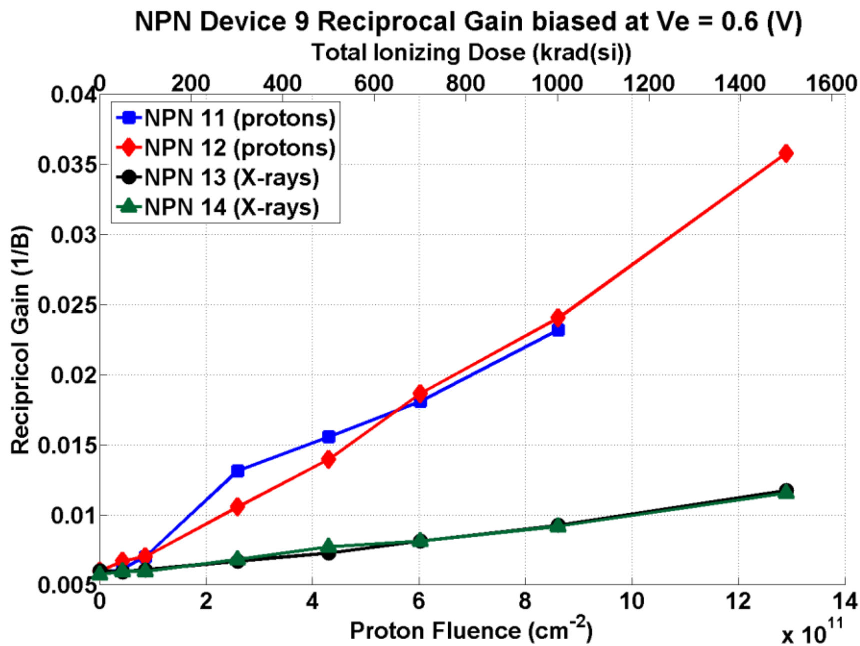

Figure 3-6: Reciprocal gain plot of four NPN devices the same size. Note the slopes are similar to the values in Figure 3-5. The last data point for NPN 11 is omitted due to device failure.

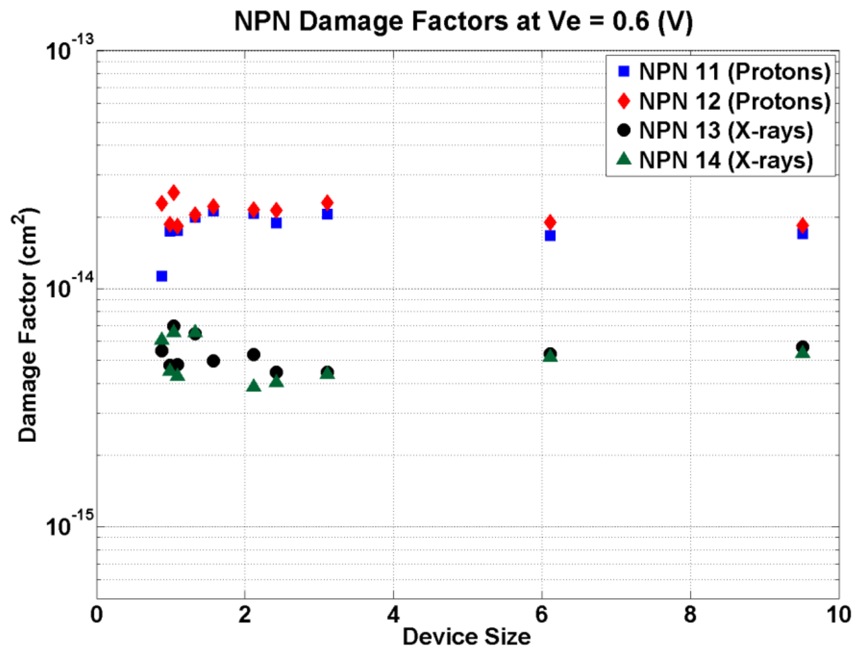

Figure 3-7: NPN BJT damage factors at 0.6 V V_{BE} bias.

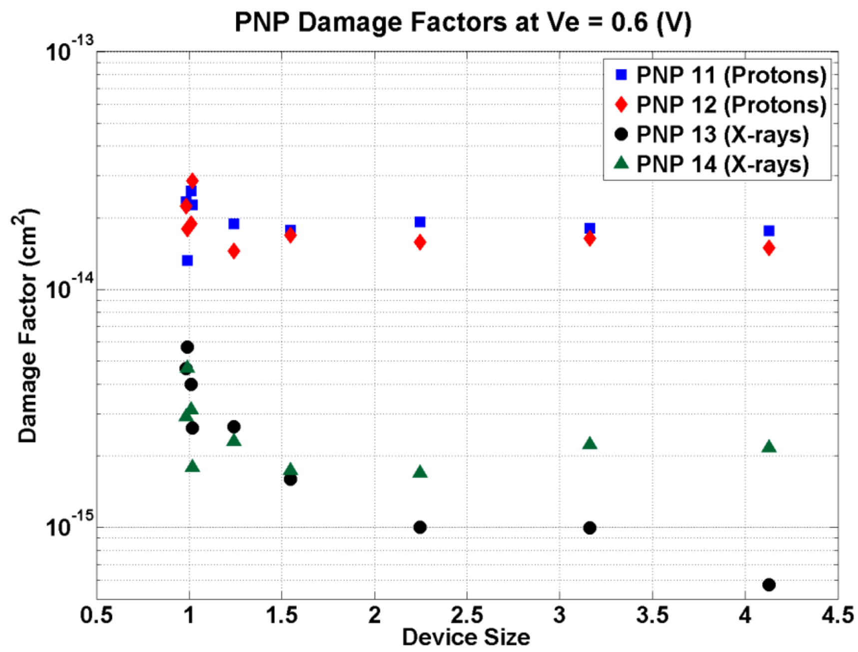

Figure 3-8: PNP BJT damage factors at 0.6 V V_{BE} bias.

3.3 Correlating Ionization and Displacement Damage

The calculated slope for each device in Figure 3-5 and Figure 3-6 is the damage factor (K) for that device at a bias of 0.6 V. Damage factor was then calculated for each device at each voltage step from 0.4 to 0.9 V as shown in Figure 3-9. While the damage factor changes depending on the emitter-base bias, the approximate ratio between the proton damage factors and the X-ray damage factors does not. Once damage factors have been calculated, they can be used to determine the amount of displacement damage caused by protons.

It has been demonstrated that the effects of 10 keV X-rays are similar to those produced by ~20 MeV protons. This is because the mass-stopping power of the secondary electrons produced by the X-rays is approximately the same as that of the protons, resulting in similar charge yields as shown in Figure 3-10 and Figure 3-11 [13]. Assuming the charge yield for ionization produced by 10 keV X-rays and 20 MeV protons is equivalent, a charge yield ratio (CYR) can be calculated from Figure 3-11 using the following equation:

$$CYR = \frac{Charge\ Yield_{\text{experimental}\,protons}}{Charge\ Yield_{20\ MeV\ protons}}$$

Using this concept, the 4 MeV protons used in this experiment have a mass stopping power that is about 2.5 times greater than that of the secondary electrons produced by10 keV X-rays or 20 MeV protons. The charge yield is about 0.35 for 20 MeV protons and 0.2 for 4 MeV protons, giving a CYR of 1.75. With a CYR, it is possible to show a quantifiable amount of displacement damage caused by protons. Since this damage is manifested as excess base current in BJTs, it can be described by the following equation:

$$\Delta I_{B\ (DD,protons)} = \Delta I_{B\ (total,protons)} - \left(\Delta I_{B\ (TID,X-rays)} \times CYR\right)$$

where ΔI_B is excess base current. An alternative way to quantify the amount of displacement damage due to protons is by using a damage factor ratio.

A percentage of ionizing damage due to protons can be calculated using a ratio with X-ray damage factors (K_X) as a numerator and proton damage factors (K_P) as a denominator. Multiplying this ratio by CYR will give a damage factor ratio (DFR) at each bias:

$$Damage\ Factor\ Ratio = \frac{K_{X,V_{BE}}}{K_{P,V_{BE}}} \times CYR$$

Once a DFR has been calculated, it can be multiplied by ΔI_B or $\Delta\beta$ to determine the percentage of damage due to ionization.

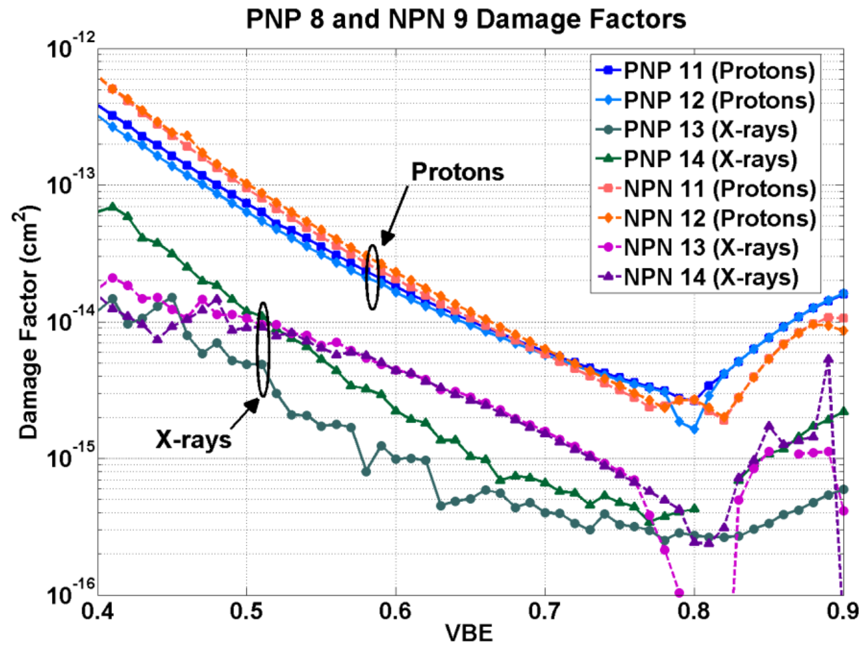

Figure 3-9: Damage factors for four NPN and four PNP devices that are similarly sized**.**

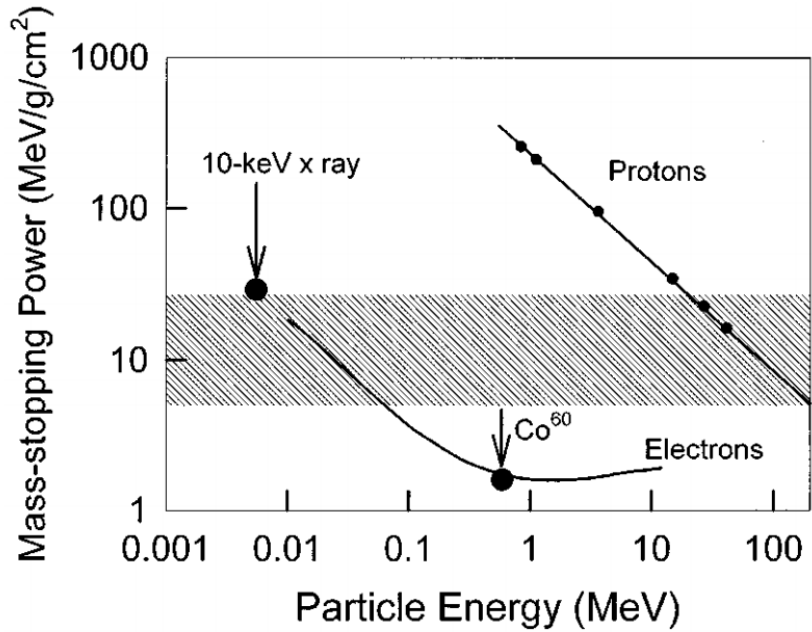

Figure 3-10: Mass-stopping powers versus particle energy for protons, electrons, and secondary electrons generated by 10 keV X-rays and 1.25 MeV Co-60 gamma ray photons. Shaded area corresponds to proton energies used by Schwank *et al*. and proton and electron data are from Oldham *et al* [13], [36].

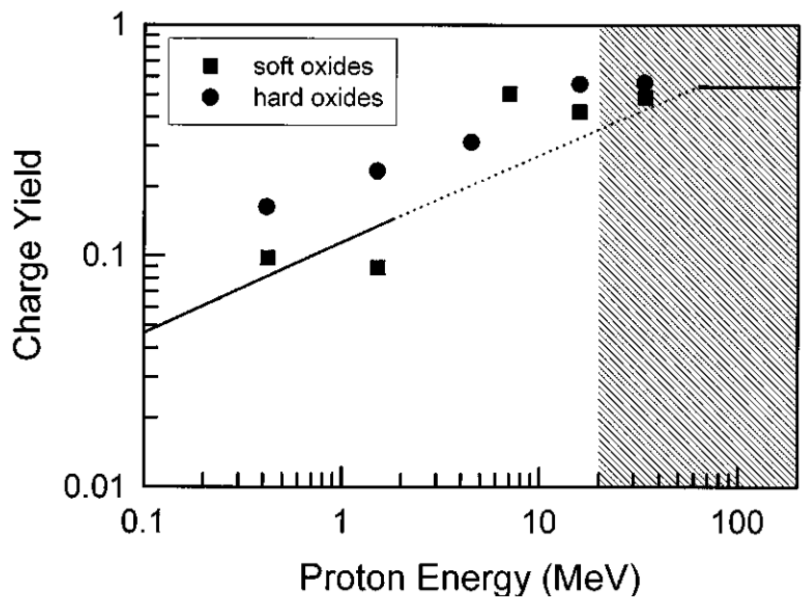

Figure 3-11: Charge yield for protons compared to proton energy. Shaded area corresponds to proton energies used by Schwank *et al*. and original plot from Oldham *et al* [13], [36]. For the charge yield experiments, n-channel transistors were irradiated with the gates grounded.

Damage factor ratio was calculated for every bias point from 0.4 V to 0.9 V is shown in Figure 3-12. In this figure, the space below the plotted line represents the percentage of damage caused by ionization due to protons and the space above the plotted lines represents the percentage of displacement damage. The PNP BJT data shows a consistent ratio of 5-10% ionization damage and the NPN BJT data shows a range from 2-15% ionization damage with the higher amount of ionization damage between 0.53 V and 0.78 V. Plots for other sized devices showed similar results. The difference in NPN BJT ionization is most likely due to the spreading of the depletion region over the p-type base due to extra oxide charge. This shows that these calculations are highly dependent on device geometry. This is consistent with research that has shown the dependence of radiation response on a variety of factors including neutral base width, base depth, base doping, emitter doping, and oxide thickness [3]. Since the dimensions of the devices used for this experiment are not well known, these calculations, if applied to other devices, should only be used as a screen for displacement damage.

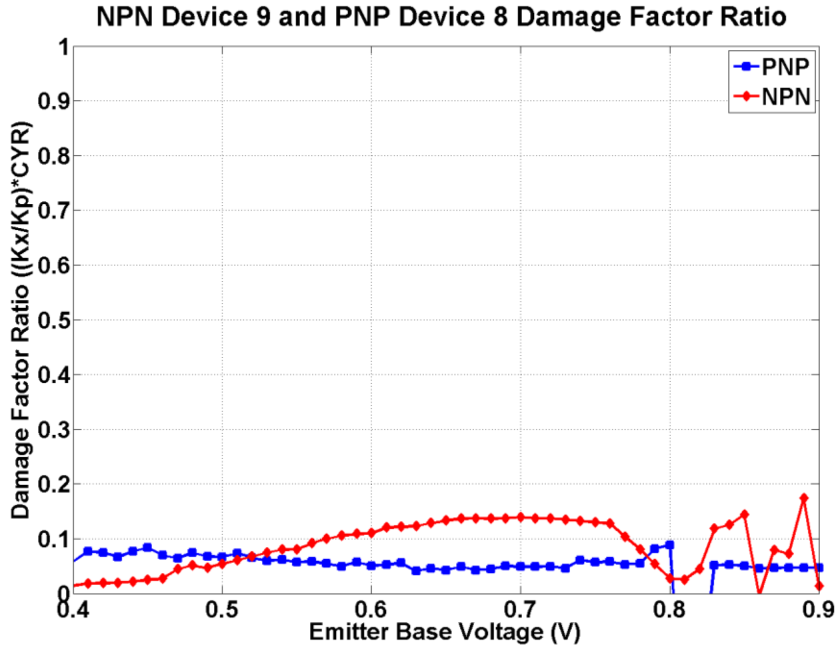

Figure 3-12: Damage factor ratio with charge yield correction factor for similarly sized NPN and PNP BJTs.

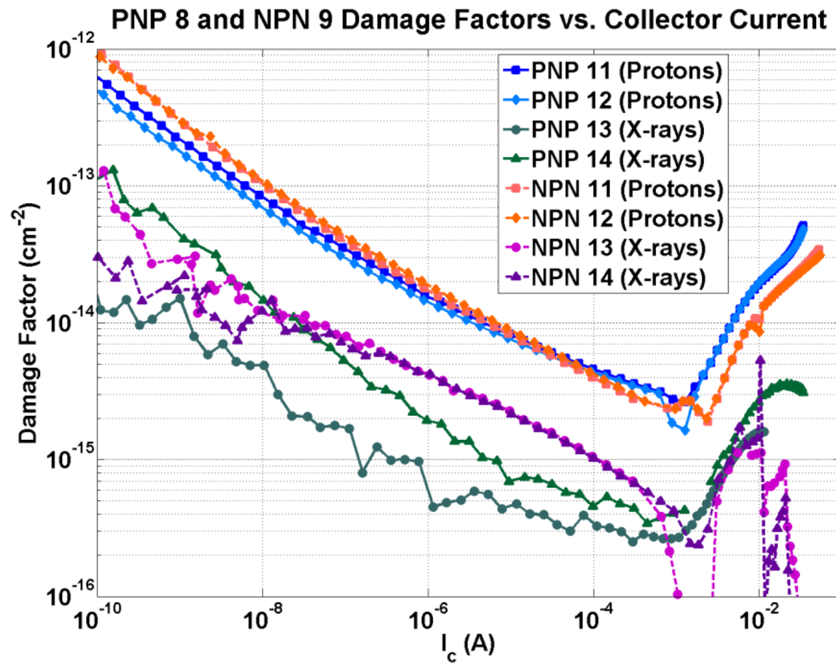

Figure 3-13: Damage factors for the same four NPN and four PNP BJTs as shown in Figure 1-3 using collector current as the abscissa for easy comparison to the similar plot from Summers et al.[16].

3.4 Comparison with Existing Work

A comparison to Summers *et al.* can be made by plotting damage factors versus collector current for these data, as shown in Figure 3-13. A similar plot is shown from Summers *et al.* in Figure 1-3 of this thesis. The numbers for proton irradiation here are within the same order of magnitude as the numbers given by that plot. Using a current bias where maximum gain degradation occurs the different damage factors can be compared. For example, the damage factor given at a collector currents bias of 1 µA for this experiment is 1.95×10^{-14} cm^2 for the NPN BJTs. This is compared to the ~1.5×10^{-14} cm^2 shown for a 2N2222A NPN BJT at 500 µA irradiated with 3.7 MeV protons [16]. However, the damage factor given at a collector currents bias of 1 µA for the PNP BJT is 1.86×10^{-14} cm^2 and the damage factor for a 2N2907A at peak gain at 50 mA is ~2×10^{-15} [16]. Besides the small difference in proton energy from 3.7 MeV to 4 MeV, most likely, these differences are due to differences in the processes with which the chips were made. Furthermore, Summers *et al.* claim that PNP technology will always have a higher damage factor than NPN technology [16]. A quick look at Figure 3-13 will show that the NPN damage factors are actually higher than the PNP damage factors. Numbers are similar here for both NPN and PNP BJTs in the TI technology, supporting work done by Barnaby *et al.* discussing the effects different sizing parameters have on radiation response [29].

In 2001, Barnaby *et al*. claimed that ionization damage accounted for about 20% of damage caused by 200 MeV protons, as shown in Figure 2-2. However, this work assumed charge yields from 10 keV X-rays and 200 MeV protons are similar and did not scale the percentage with charge yield [28]. Charge yield for 200 MeV protons is about 1.5 greater than 20 MeV protons meaning that ionization due to protons is closer to 30%.

Conclusions

The goal of this work was to determine if protons could be used to determine a device's tolerance to displacement damage as a convenient and inexpensive method to obtain a reasonable preliminary estimate. Through experiments done with 4 MeV protons and 10 keV X-rays, this was accomplished. Due to the proton being a charged particle, relevant mechanisms of both displacement damage and ionization damage were discussed to show their individual effects. This was followed by a discussion of the effects of protons, their mechanisms, and calculations related to their use in irradiating parts. Finally, experimental data showed that protons can be used to estimate a rough amount of displacement damage.

Due to the amount of dependence on process variation to determine the ratio of displacement to ionizing damage, it is not a simple task to determine the exact amount of displacement damage caused by proton irradiation. However, this thesis has shown that if compared with X-ray irradiation of the same device, it is possible to get a rough estimate of how much damage caused by protons is due to displacement damage. Finding the damage factors due to both protons (K_P) and X-rays (K_X) and finding a ratio, K_X/K_P, to describe the relationship accomplishes this. Multiplying the ratio by the proton damage will give a rough estimate of the amount of displacement damage caused. From this, it is possible to use protons to screen for displacement damage; however, if more precise results are needed, it is necessary to irradiate a part with neutrons to get a more precise displacement damage measurement. Alternatively, if device dimensions are known, it is possible using the model created by Barnaby *et al.* to calculate the amount of displacement damage caused by protons. Ultimately, this research shows that protons can be used as a cheap and quick alternative to neutrons to screen for displacement damage.

References

[1] S. Glasstone and P. J. Dolan, *The effects of nuclear weapons*, 3rd ed. Washington, D.C.: United States Department of Defense and the Energy Research and Development Administration, 1977.

[2] E. Bielejec, G. Vizkelethy, N. R. Kolb, D. B. King, and B. L. Doyle, "Damage Equivalence of Heavy Ions in Silicon Bipolar Junction Transistors," *IEEE Trans. Nucl. Sci.*, vol. 53, no. 6, pp. 3681–3686, Dec. 2006.

[3] H. J. Barnaby, "Characterization and Modeling of Proton Radiation Effects in Linear Bipolar Devices and Circuits," Vanderbilt University, Nashville, TN, 2002.

[4] R. D. Schrimpf, "Physics and Hardness Assurance for Bipolar Technologies." in IEEE Nucl. Space Radiation Effects Conf. Short Course Notes, Jul-2001.

[5] R. D. Schrimpf, "Recent advances in understanding total-dose effects in bipolar transistors," *IEEE Trans. Nucl. Sci.*, vol. 43, no. 3, pp. 787–796, Jun. 1996.

[6] K. F. Galloway, R. L. Pease, R. Schrimpf, and D. W. Emily, "From Displacement Damage to ELDRS: Fifty Years of Bipolar Transistor Radiation Effects at the NSREC," *IEEE Trans. Nucl. Sci.*, vol. 60, no. 3, pp. 1731–1739, Jun. 2013.

[7] J. R. Srour, C. J. Marshall, and P. W. Marshall, "Review of displacement damage effects in silicon devices," *IEEE Trans. Nucl. Sci.*, vol. 50, no. 3, pp. 653–670, Jun. 2003.

[8] A. Wu, R. D. Schrimpf, H. J. Barnaby, D. M. Fleetwood, R. L. Pease, and S. L. Kosier, "Radiation-induced gain degradation in lateral PNP BJTs with lightly and heavily doped emitters," *IEEE Trans. Nucl. Sci.*, vol. 44, no. 6, pp. 1914–1921, Dec. 1997.

[9] D. M. Schmidt, D. M. Fleetwood, R. D. Schrimpf, R. L. Pease, R. J. Graves, G. H. Johnson, K. F. Galloway, and W. E. Combs, "Comparison of ionizing-radiation-induced gain degradation in lateral, substrate, and vertical PNP BJTs," *IEEE Trans. Nucl. Sci.*, vol. 42, no. 6, pp. 1541–1549, Dec. 1995.

[10] R. L. Pease, F. N. Coppage, and E. D. Graham, "Dependence of ionizing radiation induced hFE degradation on emitter periphery," *IEEE Trans. Nucl. Sci.*, vol. 21, no. 2, pp. 41–42, Apr. 1974.

[11] R. N. Nowlin, R. D. Schrimpf, E. W. Enlow, W. E. Combs, and R. L. Pease, "Mechanisms of ionizing-radiation-induced degradation in modern bipolar devices," in *Bipolar Circuits and Technology Meeting, 1991., Proceedings of the 1991*, 1991, pp. 174–177.

[12] S. L. Kosier, A. Wei, R. D. Schrimpf, D. M. Fleetwood, M. D. DeLaus, R. L. Pease, and W. E. Combs, "Physically based comparison of hot-carrier-induced and ionizing-radiation-induced degradation in BJTs," *IEEE Trans. Electron Devices*, vol. 42, no. 3, pp. 436–444, Mar. 1995.

[13] J. R. Schwank, M. R. Shaneyfelt, P. Paillet, D. E. Beutler, V. Ferlet-Cavrois, B. L. Draper, R. . Loemaker, P. E. Dodd, and F. W. Sexton, "Optimum laboratory radiation source for hardness assurance testing," *IEEE Trans. Nucl. Sci.*, vol. 48, no. 6, pp. 2152–2157, Dec. 2001.

[14] S. Wood, N. J. Doyle, J. A. Spitznagel, W. J. Choyke, R. M. More, J. N. McGruer, and R. B. Irwin, "Simulation of Radiation Damage in Solids," *IEEE Trans. Nucl. Sci.*, vol. 28, no. 6, pp. 4107–4112, Dec. 1981.

[15] G. C. Messenger and J. P. Spratt, "The Effects of Neutron Irradiation on Germanium and Silicon," *Proc. IRE*, vol. 46, no. 6, pp. 1038–1044, Jun. 1958.

[16] G. P. Summers, E. A. Burke, C. J. Dale, E. A. Wolicki, P. W. Marshall, and M. A. Gehlhausen, "Correlation of Particle-Induced Displacement Damage in Silicon," *IEEE Trans. Nucl. Sci.*, vol. 34, no. 6, pp. 1133–1139, Dec. 1987.

[17] E. . Burke, "Energy Dependence of Proton-Induced Displacement Damage in Silicon," *IEEE Trans. Nucl. Sci.*, vol. 33, no. 6, pp. 1276–1281, Dec. 1986.

[18] C. J. Dale, P. W. Marshall, E. . Burke, G. P. Summers, and E. A. Wolicki, "High energy electron induced displacement damage in silicon," *IEEE Trans. Nucl. Sci.*, vol. 35, no. 6, pp. 1208–1214, Dec. 1988.

[19] I. Jun, M. . Xapsos, S. R. Messenger, E. . Burke, R. J. Walters, G. P. Summers, and T. Jordan, "Proton nonionizing energy loss (NIEL) for device applications," *IEEE Trans. Nucl. Sci.*, vol. 50, no. 6, pp. 1924–1928, Dec. 2003.

[20] S. R. Messenger, E. . Burke, G. P. Summers, M. . Xapsos, R. J. Walters, E. M. Jackson, and B. D. Weaver, "Nonionizing energy loss (NIEL) for heavy ions," *IEEE Trans. Nucl. Sci.*, vol. 46, no. 6, pp. 1595–1602, Dec. 1999.

[21] H. S. Hajghassem, J. R. Yeargan, W. D. Brown, and J. G. Williams, "Modelling the effects of neutron radiation on the Gummel-Poon parameters for bipolar NPN transistors," *Microelectron. Reliab.*, vol. 31, no. 5, pp. 969–984, 1991.

[22] R. N. Nowlin, E. W. Enlow, R. D. Schrimpf, and W. E. Combs, "Trends in the total-dose response of modern bipolar transistors," *IEEE Trans. Nucl. Sci.*, vol. 39, no. 6, pp. 2026–2035, Dec. 1992.

[23] S. L. Kosier, R. D. Shrimpf, R. N. Nowlin, D. M. Fleetwood, M. DeLaus, R. L. Pease, W. E. Combs, A. Wei, and F. Chai, "Charge separation for bipolar transistors," *IEEE Trans. Nucl. Sci.*, vol. 40, no. 6, pp. 1276–1285, Dec. 1993.

[24] R. L. Pease, "Total ionizing dose effects in bipolar devices and circuits," *IEEE Trans. Nucl. Sci.*, vol. 50, no. 3, pp. 539–551, Jun. 2003.

[25] G. W. Neudeck, *The bipolar junction transistor*, 2nd ed. Reading, Mass: Addison-Wesley, 1989.

[26] A. Wei, S. L. Kosier, R. D. Schrimpf, W. E. Combs, and M. DeLaus, "Excess collector current due to an oxide-trapped-charge-induced emitter in irradiated NPN BJT's," *IEEE Trans. Electron Devices*, vol. 42, no. 5, pp. 923–927, May 1995.

[27] S. L. Kosier, W. E. Combs, A. Wei, R. D. Schrimpf, D. M. Fleetwood, M. DeLaus, and R. L. Pease, "Bounding the total-dose response of modern bipolar transistors," *IEEE Trans. Nucl. Sci.*, vol. 41, no. 6, pp. 1864–1870, Dec. 1994.

[28] H. J. Barnaby, R. D. Schrimpf, A. Sternberg, V. Berthe, C. R. Cirba, and R. L. Pease, "Proton radiation response mechanisms in bipolar analog circuits," *IEEE Trans. Nucl. Sci.*, vol. 48, no. 6, pp. 2074–2080, Dec. 2001.

[29] H. J. Barnaby, S. K. Smith, R. D. Schrimpf, D. M. Fleetwood, and R. L. Pease, "Analytical model for proton radiation effects in bipolar devices," *IEEE Trans. Nucl. Sci.*, vol. 49, no. 6, pp. 2643–2649, Dec. 2002.

[30] J. P. Raymond and E. L. Petersen, "Comparison of Neutron, Proton and Gamma Ray Effects in Semiconductor Devices," *IEEE Trans. Nucl. Sci.*, vol. 34, no. 6, pp. 1621–1628, Dec. 1987.

[31] R. L. Pease, E. W. Enlow, G. L. Dinger, and P. Marshall, "Comparison of Proton and Neutron Carrier Removal Rates," *IEEE Trans. Nucl. Sci.*, vol. 34, no. 6, pp. 1140–1146, Dec. 1987.
[32] G. P. Summers, E. . Burke, P. Shapiro, S. R. Messenger, and R. J. Walters, "Damage correlations in semiconductors exposed to gamma, electron and proton radiations," *IEEE Trans. Nucl. Sci.*, vol. 40, no. 6, pp. 1372–1379, Dec. 1993.
[33] B. G. Rax, A. Johnston, and C. . Lee, "Proton damage effects in linear integrated circuits," *IEEE Trans. Nucl. Sci.*, vol. 45, no. 6, pp. 2632–2637, Dec. 1998.
[34] B. G. Rax, A. Johnston, and T. Miyahira, "Displacement damage in bipolar linear integrated circuits," *IEEE Trans. Nucl. Sci.*, vol. 46, no. 6, pp. 1660–1665, Dec. 1999.
[35] D. M. Schmidt, A. Wu, R. D. Schrimpf, D. M. Fleetwood, and R. L. Pease, "Modeling ionizing radiation induced gain degradation of the lateral PNP bipolar junction transistor," *IEEE Trans. Nucl. Sci.*, vol. 43, no. 6, pp. 3032–3039, Dec. 1996.
[36] T. R. Oldham, "Analysis of Damage in MOS Devices for Several Radiation Environments," *IEEE Trans. Nucl. Sci.*, vol. 31, no. 6, pp. 1236–1241, Dec. 1984.
[37] R. Jerome, M. Sun, J. Baylor, and S. Parks, "Advanced Complementary Bipolar Processes on Bonded-SOI Substrates Optimize Performance for High Voltage Precision Analog Applications." Intersil Corporation.